



JAEA-Research

2006-002



JP0650292

## Current Profiles and Major Disruptions in a Lower-Hybrid Current Drive Tokamak

Kazuya UEHARA and Takashi NAGASHIMA\*

Tokamak Experiment Group  
Fusion Research and Development Directorate

February 2006

Japan Atomic Energy Agency

日本原子力研究開発機構

# JAEA-Research

本レポートは日本原子力研究開発機構が不定期に刊行している研究開発報告書です。  
本レポートの全部または一部を複写・複製・転載する場合は下記にお問い合わせ下さい。

〒319-1195 茨城県那珂郡東海村白方白根2-4

日本原子力研究開発機構 研究技術情報部 研究技術情報課

Tel.029-282-6387, Fax.029-282-5920

This report was issued subject to the copyright of Japan Atomic Energy Agency.

Inquiries about the copyright and reproduction should be addressed to :

Intellectual Resources Section,

Intellectual Resources Department

2-4, Shirakata-shirane, Tokai-mura, Naka-gun, Ibaraki-ken, 319-1195, JAPAN

Tel.029-282-6387, Fax.029-282-5920

## Current Profiles and Major Disruptions in a Lower-Hybrid Current Drive Tokamak

Kazuya UEHARA and Takashi NAGASHIMA \*

Division of Advanced Plasma Research  
Fusion Research and Development Directorate  
Japan Atomic Energy Agency  
Naka-shi, Ibaraki-ken, Japan

(Received January 4 , 2006)

**Summary** – The radial rf current profile of the lower-hybrid current drive tokamak is estimated using an rf power damping model for various Gaussian type  $n_z$  spectra ( $= \exp(-(n_z - n_{zc})^2/h_z)$ ), and condition for stability against major disruptions are examined using the criterion of the tearing mode instability. The value of  $n_{zc}$  determines the spatial damping of the rf power and the resultant rf current profile. The value of  $h_z$  determines the extent of the damping of the rf power and the resultant absolute value of the rf current. The peaking and flattening characteristics of current profile which is free from disruption are obtained when the rf power is not damped at the boundary region and when the extent of damping is relatively small even if the rf power begins to damp at regions close to boundaries, where the rf spectrum has relatively large phase velocity and is not so broad.

**Keywords:** Lower-hybrid Current Drive, Current Profile, Major Disruptions, Tearing Mode Instability, Spatial Damping

---

\* Nippon Advanced Technology Co., Ltd.

## 低域混成波による電流駆動トカマクにおける電流分布とデスラプション

日本原子力研究開発機構

核融合研究開発部門先進プラズマ研究開発ユニット

上原 和也・永島 孝\*

(2006 年 1 月 4 日受理)

低域混成波による電流駆動トカマクにおける径方向の電流分布が、色々なガウス型の  $n_z$  スペクトル( $= \exp(-(n_z - n_{zc})^2/h_z)$ )に対して、準線形理論と rf 減衰モデルを用いて評価され、メジャーデスラプションに対して安定な条件がテアリング不安定の基準を用いて調べられた。進行波低域混成波  $n_z$  スペクトルの中心屈折率  $n_{zc}$  は rf パワーの空間減衰を決めていて、電流分布に直接関与している。 $n_z$  スペクトルのシャープさを決める  $h_z$  は rf パワーの空間減衰の程度を決めていて、駆動電流の大きさの絶対値を決めている。メジャーデスラプションはテアリング不安定の 2 つの磁気島が接触する際に起こるという基準が適用され、色々な  $n_{zc}$  や  $h_z$  を持つ RF スペクトルの波に対して、駆動される電流分布が計算され、このような電流分布をもったトカマクがデスラプションに対して安定となるかどうか調べられている。

---

那珂核融合研究所 (駐在) : 〒311-0193 茨城県那珂市向山 801-1

\*日本アドバンス・テクノロジー

## Contents

1. INTRODUCTION-----	1
2. EVALUATION OF CURRENT PROFILE DUE TO RF POWER DAMPING MODEL-----	2
3. JUDGMENT OF DISRUPTIVE INSTABILITY-----	5
4. DISCUSSION AND CONCLUSION-----	6
ACKNOWLEDGMENTS-----	8
REFERENCES-----	9

## 目 次

1. 序論-----	1
2. RF 減衰モデルに依る電流分布の評価-----	2
3. デスラプションの判定-----	5
4. 討論と結論-----	6
謝辞-----	8
参考文献-----	9

This is a blank page.

## 1. INTRODUCTION

Disruptive instability has been said to be most harmful in the plasma discharge stage of the inductive current drive (ICD) tokamak. However, with appearance of the non-inductive current drive (NICD) tokamak driven by an rf traveling wave<sup>1-5)</sup>, the possibility of becoming free from disruptive instability have been often pointed out both theoretically<sup>6-8)</sup> and experimentally<sup>9-10)</sup>. Theoretically, Yoshioka and Reiman have calculated that the presence of a lower-hybrid current can strongly suppress the growth of a magnetic island<sup>7, 8)</sup>. Experimentally, the observation of MHD activity indicates that the presence of rf driven current suppresses the growth rate of the MHD mode and allows stable low  $q(a)$  discharge (as low as 2)<sup>9, 19)</sup>. On the other hand, Waddel et al., found that a nonlinear interaction between  $m/n=2/1$  and  $m/n=3/2$  tearing modes causes magnetic disruption, where  $m$  is the poloidal mode number and  $n$  is the toroidal mode number. The plasma current generated by the rf wave seems to produce the same poloidal magnetic field<sup>11)</sup> and in resultant the same rotational transform produced together with the toroidal field, as that in the ICD tokamak. Thus, we will apply the criterion used in the ICD tokamak to the NICD tokamak as well.

Recently, in discussions about the controlling the current profile to get high beta plasma and to suppress the MHD activity, profile consistency is frequently raised<sup>12)</sup>. According to this scheme of thought, it is very difficult to control the current profile independently of the electron temperature since the current organizes itself into a certain secret channel. It is also pointed out that the deposition profile due to the power input by further heating cannot only affect current profile but also must affect electron temperature<sup>13)</sup>. However, it seems that only in the NICD by an rf traveling wave can realize a desirable current profile since the current profile in the NICD is determined by the rf wave having the higher phase velocity with low collisionality. Thus, the profile control by the LHCD is most realistic method to control the current profile.

This paper gives a method for derivation of the current profile of the lower-hybrid current drive tokamak using quasi-linear Landau damping, a discussion of the stability of the NICD tokamak using the quasi-linear Landau damping model, and a discussion of the stability of the NICD tokamak using the criterion of tearing mode instability. In section 2, the current profile of the lower-hybrid current drive tokamak based on a

quasi-linear theory is calculated using rf power damping model. In section 3, the stability of this tokamak is evaluated using a three dimensional non-linear code based on the tearing mode. In section 4, discussion and conclusions are presented.

## 2. EVALUATION OF CURRENT PROFILE DUE TO RF POWER DAMPING MODEL

In order to evaluate the stability against disruptive instability in tokamak, we must get a plausible rf current profile in the radial direction. If we consider the propagation of the wave in the radial direction, the rf wave may be Landau damped strongly near the center since the quasi-linear diffusion coefficient  $D_{QL}$  in the velocity space becomes small and the quasi-linear damping rate  $k_{QL}$  becomes closer to linear at positions approaching the center. We want to estimate the rf current radial profile using an rf power damping model having a slab geometry. The characterization of the rf current after the quasi-linear plateau is formed is well-known, expressed as

$$J_{rf} = nv_{the} \int_{-\infty}^{\infty} \omega f(\omega) d\omega \quad (1)$$

where

$$f(\omega) = c \exp\left(\int \frac{-\omega}{1 + \omega^2 D_{QL}} d\omega\right) \quad (2)$$

The distribution function  $f(\omega)$  is in the stationary quasi-linear plateau and  $\omega$  is the phase velocity in the toroidal direction  $v_z$  normalized by the electron thermal velocity  $v_{the}$ , so that,  $\omega = v_z/v_{the}$ . The value of  $D_{QL} \neq 0$  for  $\omega < \omega_1$ ,  $\omega > \omega_2$  and  $D_{QL} = 0$  for  $\omega_1 < \omega < \omega_2$ , where  $\omega_1$  and  $\omega_2$  are the higher and lower value of the Gaussian wave spectrum, respectively, and  $D_{QL}$  is the quasi-linear diffusion coefficient in the velocity space, expressed as

$$D_{QL} = \frac{ne^2}{m_e^2} \frac{E_{rf}^2}{v_{zc} \Delta k_z v_0 v_{the}} \quad (3)$$



, where  $e$  and  $m_e$  are the charge and mass of electrons, respectively,  $v_{zc}$  is the central velocity of the wave spectrum,  $\Delta k_z$  is the difference of the wave number,  $\nu_0 (= 3\omega_{pe}^4 \ln \Lambda / 4\pi n_e v_{the}^3)$  is the electron-electron collision frequency between bulk electrons of density  $n_e$ ,  $\omega_{pe}$  is the electron plasma frequency, and  $\ln \Lambda$  is the Coulomb logarithm. The  $f(\omega)$  is normalized so that  $\int_{-\infty}^{\infty} f(\omega) d\omega = 1$ . The relation  $E_{rf}$  and the local rf power  $P_{rf}$  in a resonance cone can be computed as follows<sup>14)</sup>.

$$P_{rf} = \frac{E_{rf}^2}{8\pi} \left(1 + \frac{k_x^2}{k_z^2}\right) \left(1 + \frac{\omega_{pe}^2}{\omega_{ce}^2}\right) S \frac{r}{a} v_g \quad (4)$$

where  $k_z$  and  $k_x$  are the wave number in  $z$  and  $r$  direction :  $k_z = \omega_0 / v_z$ ,  $k_x = (\omega_{pe} / \omega_{pi}) (k_z / (\omega_0^2 / \omega_{LH}^2 - 1))^{1/2}$  and  $\omega_{ce}$  is the electron cyclotron frequency,  $S$  is the area of the wave mouth,  $a/r$  is a cylindrical focusing factor based on the correlation near the center,  $c$  is the light velocity,  $\omega_0$  is the injected rf frequency,  $\omega_{LH}$  is the lower-hybrid frequency,  $\omega_{pi}$  is the ion plasma frequency and  $v_g$  is the group velocity of the lower-hybrid wave,

$$v_g = \sqrt{\frac{\pi}{h_z} \frac{(\omega_0^2 / \omega_{LH}^2 - 1)^{3/2}}{\omega_0^2 / \omega_{LH}^2} \frac{\omega_{pi}}{\omega_{pe}}} \quad (5)$$

where  $n_{zc}$  is the central value of the Gaussian  $n_z$  spectrum. In this procedure, however, we must consider the fact that the rf power is damped in the radial direction. The local power  $P_{rf}(r, n_z)$  of the slow wave propagating in the  $r$  direction is expressed in one dimensional WKB approximation as

$$\frac{dP_{rf}(r, n_z)}{dr} = -2k_{QL} P_{rf}(r, n_z) \quad (6)$$

where  $k_{QL}$  is the spatial damping rate due to the quasi-linear effect, which is <sup>15)</sup>

$$k_{QL} = \sqrt{\frac{\pi}{8}} \frac{\omega^3}{1 + 2\omega^3 D_{QL}} e^{-\omega^2 \frac{(k_x^2 + k_z^2)^2}{k_x^2 k_z^2}} \quad (7)$$

when  $D_{QL} = 0$ , then the damping is linear so that the wave is strongly Landau damped, and when  $D_{QL} \neq 0$ , then the damping is quasi-linear so that the wave is slightly suppressed. The boundary condition in solving eq.(6) is the value at the wave guide mouth;  $P_{rfa} = (P_{rf0}/(\pi h_z)^{1/2}) \exp(-(n_z - n_{zc})^2/h_z)$  at  $r=a$ , where we assume the  $n_z$  spectrum of the slow wave to be Gaussian without making the Brambilla calculation<sup>16)</sup>, and the accessibility condition  $n_z > n_{za} = (1 + (\omega_{pe}/\omega_{ce})^2)^{1/2}$  should be satisfied for  $r < a$ . The

integration must be performed over all value of  $n_z$  in solving eq.(6) :  $\int_{-\infty}^{\infty} P_{rfa} dn_z = P_{rf0}$

where  $r=a$  and  $P_{rf} = \int_{n_{za}}^{\infty} P_{rf}(r, n_z) dn_z$  where  $r < a$ .

The procedure to obtain the radial profile of  $J_{rf}$  is as follows. Firstly, the value of  $E_{rf}$  is obtained using the value of  $P_{rf}$  in eq.(4) after above mentioned integrating with respect to  $n_z$ , then  $D_{QL}$  is obtained from eq.(3), and finally  $k_{QL}$  is obtained by eq.(7). The next step is to obtain  $P_{rf}$  a little bit to the inside using  $P_{rf}$  value a little bit to the outer side and so on. Thus, the radial profiles of  $P_{rf}$ ,  $E_{rf}$ ,  $D_{QL}$ ,  $k_{QL}$  and  $J_{rf}$  are obtained by using eq.(1) through eq.(2) step by step from the outer side to the inner side. Figures 1 and 2 show the radial profiles of  $P_{rf}$  and  $E_{rf}$  in the case of  $h_z=5$  and  $n_{zc}=4$  putting  $n_{zc}$  and  $h_z$  as a parameter, respectively. Figures 3 and 4 show the radial profile of  $J_{rf}$  with the same parameters as Figs 1 and 2. It is seen that the rf current distribution is hollow when  $n_{zc}$  is relatively large and peaks at the center when  $n_{zc}$  is relatively small and that the absolute value of  $J_{rf}$  becomes large with increase of  $h_z$ . The large  $h_z$  corresponds to a wide  $n_z$  spectrum. Figures 4 and 5 show the radial profile of  $J_{rf}$  in the case of  $n_{zc}=4$  and  $n_{zc}=3$ , respectively putting  $h_z$  as a parameter. The case of  $n_{zc}=4$  is an example of a hollow current profile and the case of  $n_{zc}=3$  is one of a center peak current profile. It is because at  $n_{zc}=2$  case the rf power generated does not satisfy the accessibility condition that the absolute value of  $J_{rf}$  is small in Fig. 3. It should be noted that the rf current profile in the plasma column is rather flat when  $n_{zc}$  and  $h_z$  are relatively large.

### 3. JUDGMENT OF DISRUPTIVE INSTABILITY

From the theoretical point of view there are basically two schools of interaction of major disruption. In the first theory<sup>17-19)</sup>, the disruption is believed to be triggered by the onset of stochasticity indicating destruction of magnetic surfaces, which is caused by linear coupling of  $m=2$  mode to modes of other helicity (for example  $m=3$  and  $n=2$ ). Waddel et al.<sup>17)</sup>, proposed that a non-linear interaction between  $m/n=2/1$  and  $m/n=3/2$  tearing modes caused the major disruption. In the second theory<sup>20)</sup>, the disruption is viewed as the intersection of a single helicity mode ( $m=2$  and  $n=1$ ) with a limiter or a cold gas region. According to the criterion of the first theory, we estimate the stability of the NICD tokamak using the current profile estimated in the previous section.

Furth et al.<sup>21)</sup> have derived the stability conditions for cylindrical plasma with regard to tearing mode instability using the infinite conductivity equation, in which they apply the magnetic field perturbation function  $\Psi$  and evaluate the quantity of  $\Delta' = \frac{d}{dr}(\Psi_2 - \Psi_1) \big|_{r_s} / \Psi(r_s)$ , where  $\Psi_1$  and  $\Psi_2$  are functions being extended over respective ranges of  $0 < r < r_s$  and  $r_s < r < b$ , respectively. The point of  $r_s$  and  $b$  represent the value where  $F(r_s)=0$  and the position of the perfectly conducting wall, respectively, where  $F = \vec{k} \cdot \vec{B}$  as shown by Furth. Here we follow this criterion to judge the stable conditions of a lower-hybrid current drive tokamak; the tearing mode is stable for  $\Delta' < 0$  and is unstable for  $\Delta' > 0$ . At JAERI, a three dimensional non-linear code of major disruptions using the tearing mode instability model discussed here has been established<sup>22)</sup>.

The safety factor  $q$  is easily obtained using the rf current profile in the case of  $n_{zc}/h_z=4/3$ ,  $4/5$  and  $4/9$  as shown in Fig. 6. In the procedure to estimate  $q(r)$ , the following equations are used;  $q=(r/R)(B_z/B_\theta)$ ,

$$B_\theta = (4\pi \times 10^{-1}) \int_0^r j_{rf} r' dr' \quad B_z = (4\pi \times 10^{-1}) \int_0^r j_{rf} r' dr' , \quad B_z = B_{z0} R/(R+r) , \quad , \quad \text{where } j_{rf} \text{ is}$$

normalized by the total current  $I_p$ , which is given  $I_p = \int_0^a j_{rf} 2\pi r dr$ . The saturation width of the  $m/n = 2/1$  and  $m/n = 3/2$  islands ( $\omega_{21}$  and  $\omega_{32}$ ) and the resonance positions ( $r_{21}$  and  $r_{32}$ ) can be estimated if we find the profile of the safety factor, where  $\omega_{21}$  and  $\omega_{32}$

are the width of  $m/n = 2/1$  and  $m/n = 3/2$  islands, respectively. The criterion whether  $\Delta'$  is positive or negative corresponds to whether two islands may contact or not. When  $r_{21} - \omega_{21}/2 > r_{32} + \omega_{32}/2$ , the 2/1 and 3/2 islands contact, which may cause a major disruption ; this is denoted by “NO” in the

Table 1. They do not contact when  $r_{21} - \omega_{21}/2 < r_{32} + \omega_{32}/2$ , so that no major disruption occurs ; this is denoted by “YES” in the Table 1. As shown in Table 1, even the hollow profiles of large  $n_{zc}$  ( $n_{zc}/h_z=4/5$  and  $5/5$ ) may be a good curvature for a profile to be free from major disruption. However, a slightly hollow profile ( $n_{zc}/h_z=4/7$  and  $4/9$ ) having relatively small  $n_{zc}$  may be a bad curvature for a  $q$  profile, because  $h_z$  is relatively large, so that the magnetic islands at  $q=2$  and  $q=1.5$  on the rational surface contact something to be an avoided due to the danger of major disruption. In this case the current profile and  $q$  profile are both rather flat in the plasma column. However, it should be noted that the double tearing mode is not included in this calculation.

#### 4. DISCUSSION AND CONCLUSION

It should be noted that the shape of the  $n_z$  spectrum affects the spatial damping of the rf wave. As shown in Fig. 1, there are both cases where  $P_{rf}$  is damped and is not damped with approach to the center. The reason for this is the spatial damping effect of  $k_{QL}$ . The value of  $k_{QL}$  abruptly increases with increase of  $\omega$  when  $\omega < \omega_{cr}$ , where  $\omega_{cr}$  is the value where  $\partial k_{QL}/\partial r=0$ , whereas,  $k_{QL}$  abruptly decreases with increase of  $\omega$  when  $\omega > \omega_{cr}$  as shown in Fig.7. If the value of  $n_z$  is kept constant in the radial direction, the value of  $\omega$  decreases with change in  $v_{the}$  at positions closer to the center. Firstly, we consider the case where  $D_{QL}$  is constant for the sake of convenience. When  $n_{zc}$  is less than a certain value of  $n_{zcc}$ , where  $n_{zcc}=c/\omega_{cr}v_{the}$ ,  $k_{QL}$  becomes very small and  $P_{rf}$  is hardly damped at all at positions close to the center, whereas when  $n_{zc}$  is larger than  $n_{zcc}$ , then  $k_{QL}$  becomes relatively large and  $P_{rf}$  is damped at positions close to the center. Next, we consider the case that  $D_{QL}$  is not constant in the radial direction. The quantity of the variation of  $D_{QL}$  is very larger along the radial direction changing from  $10^2$  at the boundary to  $10^{-1}$  at the center<sup>23)</sup>. Furthermore, with increase of  $n_z$ ,  $D_{QL}$  becomes still smaller according to eq.(3). Thus,  $k_{QL}$  becomes larger and larger forward to the center when  $n_{zc} > n_{zcc}$ . Whether the rf current profile comes to be the

hollow type or center-peaked type depends on where  $\omega_{cr}$  locates in the plasma column. The rf power is almost completely damped when  $\omega_{cr}$  is near the boundary, and is hardly damped when  $\omega_{cr}$  is near the center. Thus, the hollow profile is observed when the electron temperature is relatively large or  $n_{zc}$  is large, whereas the center-peaked profile is observed when the electron temperature is small or  $n_{zc}$  is small. It is noted that the radial profile of the rf power damping changes with the variation of  $n_{zc}$ . The rf power is damped more at the boundary for large  $n_{zc}$  and does more at the center for small  $n_{zc}$ .

On the other hand, a large  $h_z$  means a wide  $n_z$  spectrum and this indicates that  $E_{rf}$  does not become very small even forward the center as shown in Fig. 2, which may cause the rf current to increase with large  $D_{QL}$  as shown in eq.(3). However, the extent of the spatial damping does not change with the variation of  $h_z$  as shown in Fig. 2. It should be noted that a flat rf current profile may be obtained when  $n_{zc}$  is relatively large or the electron temperature is large so that there is slightly hollow and  $h_z$  is relatively large so as to yield constant rf current. However, when  $n_{zc}$  or  $h_z$  becomes too large, the resulting bad curvature in the  $q$  profile may sometimes lead to a major disruption. Thus, a good curvature of the current profile free from major disruption can be obtained when  $n_{zc}$  is small and  $h_z$  is not very large so that there is a gentle slope of the current at the rational surfaces even in the case of relatively large  $n_z$ .

In this paper, we apply the Gaussian distribution to the rf spectrum. However, the Brambilla spectrum must be applied in practice. The shape of  $n_z$  spectrum is determined by the size (widths  $b$  and septum  $b$ ) of the grill launcher, the frequency  $f$  of the lower-hybrid wave and also the phase difference  $\Delta\phi$  with the adjacent waveguide. The calculation of the Brambilla spectrum in the case of the JT-60 lower-hybrid launcher shows that with decrease of  $b$ ,  $d$  and  $f$ , the value of  $n_z$  and  $h_z$  becomes large as shown in Fig. 8. Thus, it is necessary to select the width and the septum of the opening and the frequency of the wave to optimize the  $n_z$  spectrum so as to avoid the disruption. If we want to decrease  $h_z$  only, then the opening, the septum and also the frequency must be larger; however, by so doing  $n_{zc}$  becomes smaller. Thus, the controlling  $\Delta\phi$  is an attractive method to get the optimum rf spectrum. In the JT-60 lower-hybrid heating system, a real time feed back control of  $f$  and  $\Delta\phi$  according to the variation of plasma parameters is possible<sup>24)</sup>. Avoidance of the disruptive instability can be attained by controlling the  $f$  and  $\Delta\phi$  performance of rf hardware.

In the calculations for this paper, the case of  $h_z > 2$  was considered not to be

realistic in practice from a technological point of view.

In this paper there are some problems that must be clarified. Since the slab model is used in the calculation, the toroidal effect is not included in such factor as the variation of  $n_z$ . Therefore, it must be considered that the current profile produced by LHCD and a resultant estimation of the disruption conditions has only a qualitative meaning. Absolute value of  $n_z$  on the parameter dependence is not always correct in the calculation and these must be clarified by the exact treatment such items as the ray tracing code in the wave propagation. Since we only inserted the  $q$  profile of the lower-hybrid current drive tokamak into the non-linear code of the tearing mode, the validity of the judgment of disruptive instability must be discussed elsewhere after further study.

Recently, the JT-60 U have demonstrated to control the current profile in LHCD through the real time feed back of the phase difference<sup>25)</sup>.

In conclusion, we have shown that the  $n_z$  spectrum determines the rf current profile and  $q$  profile and as a result the stability against major disruptions. The variation of the peak value of  $n_z$  spectrum determines the spatial damping of the rf power and thus the rf current profile. In the case of large  $n_{zc}$  the rf power damps sooner at the boundary region to cause a hollow profile, and damps only a little or not at all at the center to cause a center-peaked profile in the case of small  $n_{zc}$ . The variation within the profile of  $n_z$  spectrum determines the extent of the damping of the rf power. The absolute value of the rf current becomes large for large  $h_z$ . The flattened peak current profile which is free from disruption is obtained when rf power is not damped at the boundary region and when the extent of damping is relatively small even if the rf power begins to be damped relatively close to the boundary, where the rf spectrum has relatively large phase velocity and has a profile which is not so broad.

## ACKNOWLEDGMENTS

Technical performance of the simulation by K. Hata in JAERI computer center is appreciated. We want to thank Dr. M. Azumi for his permission to use the computer code for the tearing instability.

## REFERENCES

- 1) FISCH, N. J. , Phys. Rev. Lett. **41**, 873 (1978)
- 2) YAMAMOTO, T., et al., Phys. Rev. Lett. **45**, 716 (1980)
- 3) NAKAMURA, M., et al., Phys. Rev. Lett. **47**, 1902 (1982)
- 4) LUCKHRDT, S.C., et al., Phys. Rev. Lett. **48**, 152 (1982)
- 5) BERNABEI, S. ,et al., Phys. Rev. Lett. **49**, 1255 (1982)
- 6) SHIGETA, M., et al., J. Phys. Soc. Jpn. **51**, 3012 (1981)
- 7) REIMAN, A. H., Princeton Plasma Phys. Lab. Rep. PPPL-1907 (1982)
- 8) YOSHIOKA, H., et al., Nucl. Fusion **24**, 565 (1984)
- 9) MELIN, G. ,et al., Plasma Phys. **26** 1A 123 (1984)
- 10) VAN HOUTE, D., et al., Nucl. Fusion **24**, 1985 (1984)
- 11) FISCH, N.J. & KARNEY, C. F. F. F., Phys. Rev. Lett. **54**, 897 (1985)
- 12) COPPI, B., Comment on Plasma Phys. Contr. Fusion **5**, 261 (1980)
- 13) WAGNER, F., et al., Phys. Rev. Lett. **49**, 1408 (1982)
- 14) YAMAMOTO, T., et al., J. Phys. Soc. Jpn. **48**, 1324 (1979)
- 15) YUEN, S. Y., et al., Nucl. Fusion **20**, 159 (1980)
- 16) BRAMBILLA, M., Nucl. Fusion **19**, 1343 (1979)
- 17) WADDEL, B. V., et al., Phys. Fluids **22**, 896 (1979)
- 18) WHITE, R. B., et al., Phys. Rev. Lett. **39**, 1618 (1977)
- 19) CALLEN, J. D., et al., Proc. of 7<sup>th</sup> . IAEA Int. Conf. on Plasma Phys. and Contr. Nucl. Fusion, Innsbruck, vol. I, p.415 (1978)
- 20) SYKES, A. and WESSON, J.,A., Phys. Rev. Lett. **44**, 1215 (1980)
- 21) FURTH, H. P., et al., Phys. Fluids **16**, 1054 (1973)
- 22) AZUMI, M., private communications, & KURITA, G., et al., JAERI-M 9788
- 23) UEHARA, K., J. Phys. Soc. Jpn. **53**, 2018 (1984)
- 24) UEHARA, K., et al., Fusion Eng. Design **19**, 29 (1992)
- 25) SUZUKI, T., et al., "Steady State High  $b_N$  Discharges and Real-Time Control of Current Profile in JT-60U", Proc. of 20<sup>th</sup> IAEA Fusion Energy Conference, Vilamoura (2004), IAEA-CN-116/EX/1-3

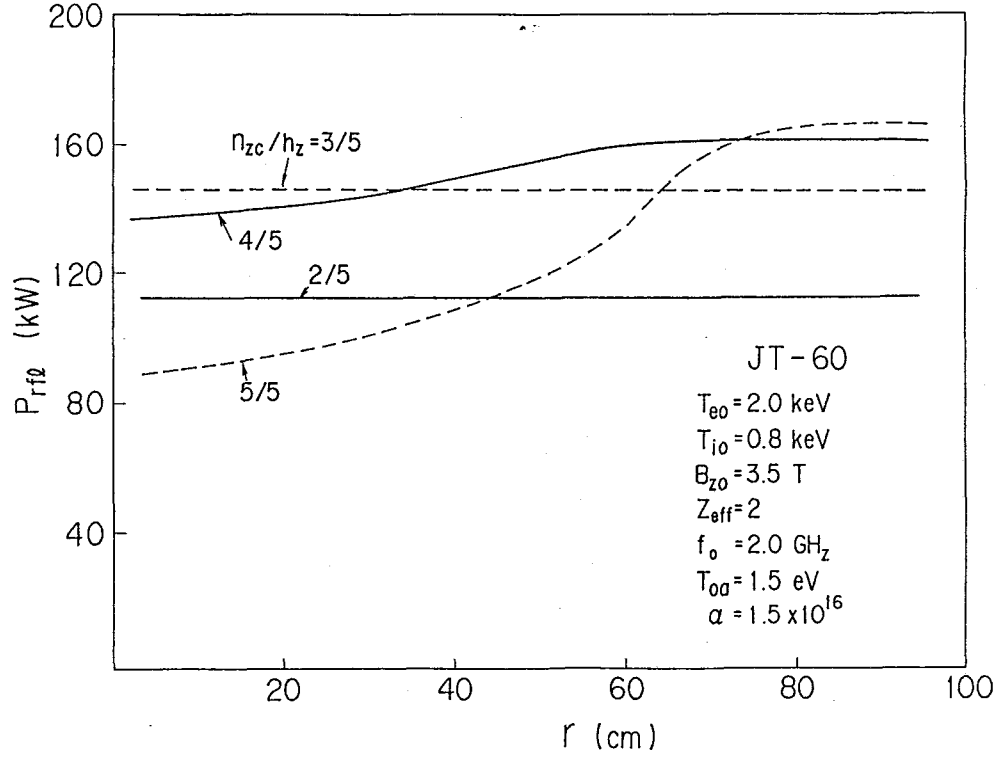


Fig. 1 The radial profile of the rf power  $P_{rf}$  at  $h_z=5$  putting  $n_{zc}$  as a parameter, where another parameters seen in figures of this paper follows after ref.[23].

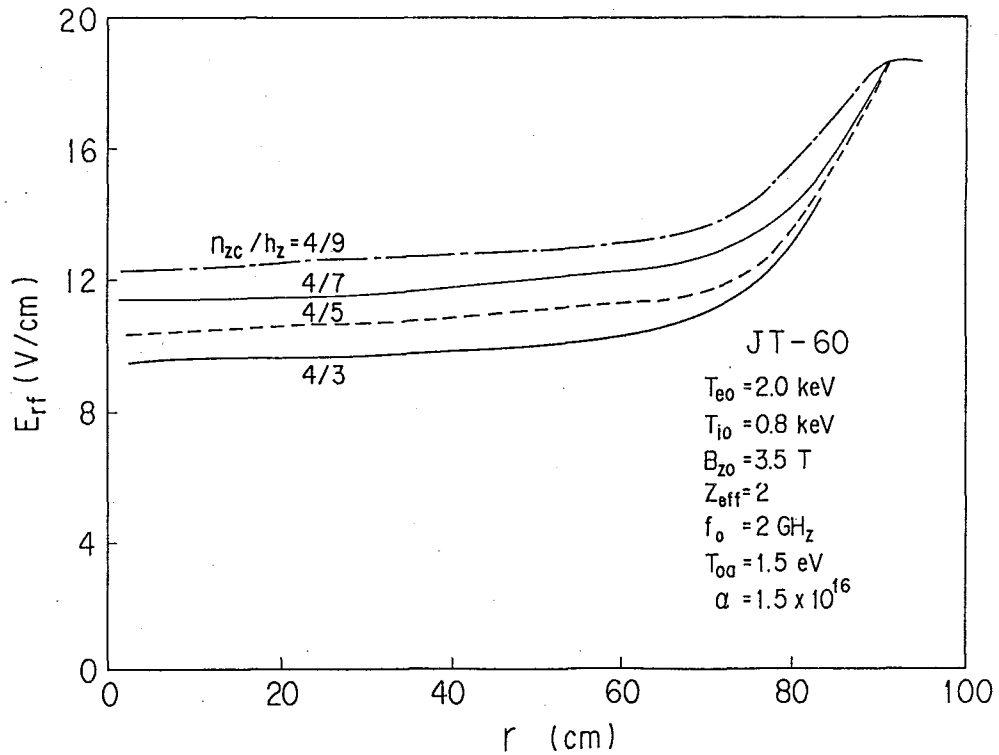


Fig. 2 The radial profile of the rf electric field  $E_{rf}$  at  $n_{zc}=4$  putting  $h_z$  as a parameter.



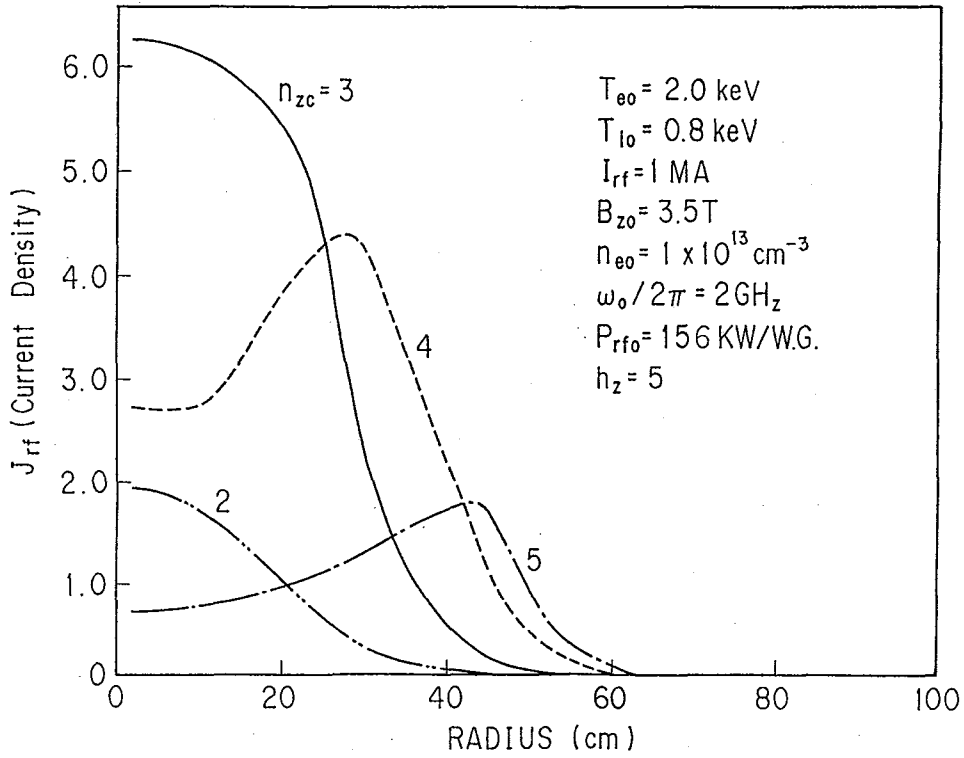


Fig. 3 The radial profile of the rf current at  $h_z=5$  putting  $n_{zc}$  as a parameter.

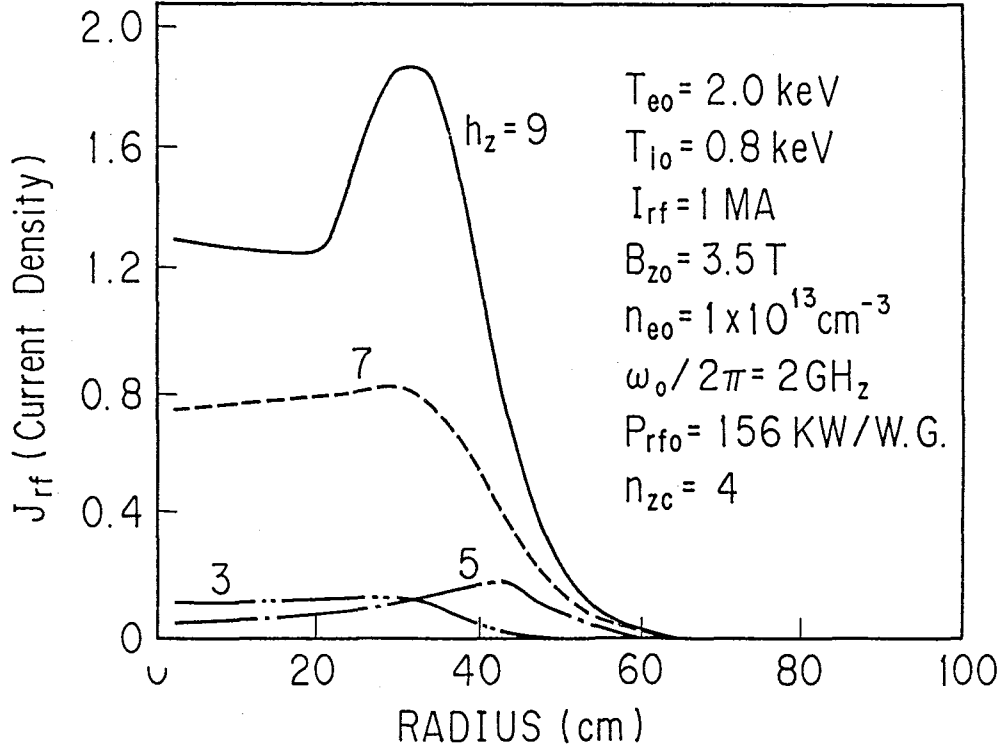


Fig. 4 The hollow type radial profile of the rf current at  $n_{zc}=4$  putting  $h_z$  as a parameter.

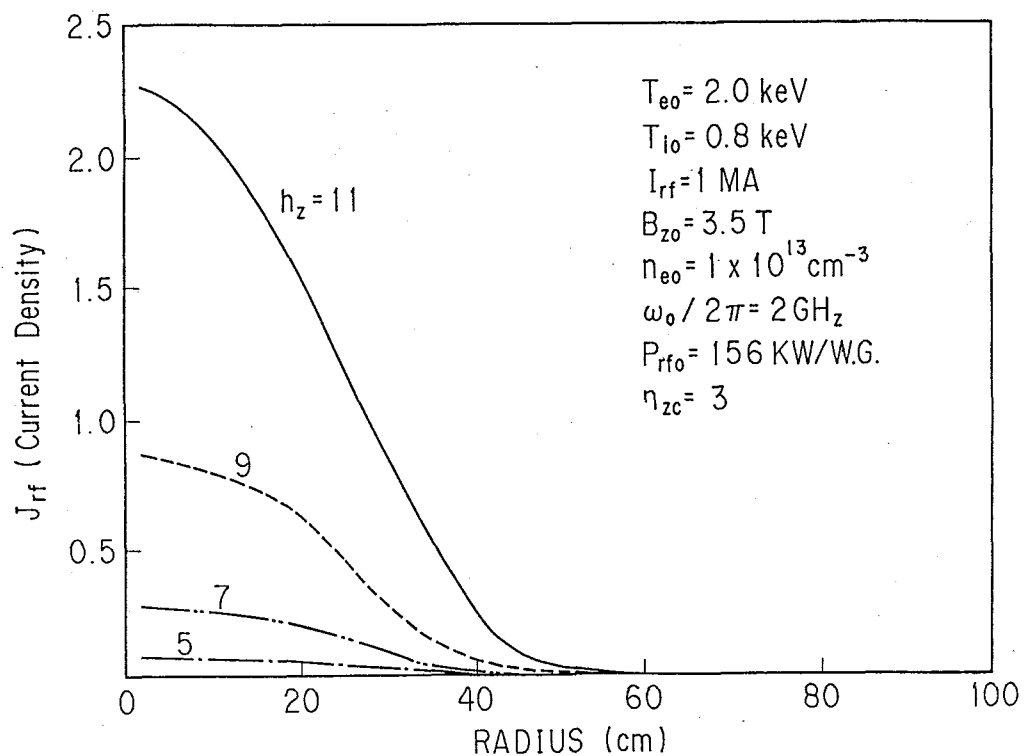


Fig. 5 The peaking type radial profile of the rf current at  $n_{zc}=4$  putting  $h_z$  as a parameter.

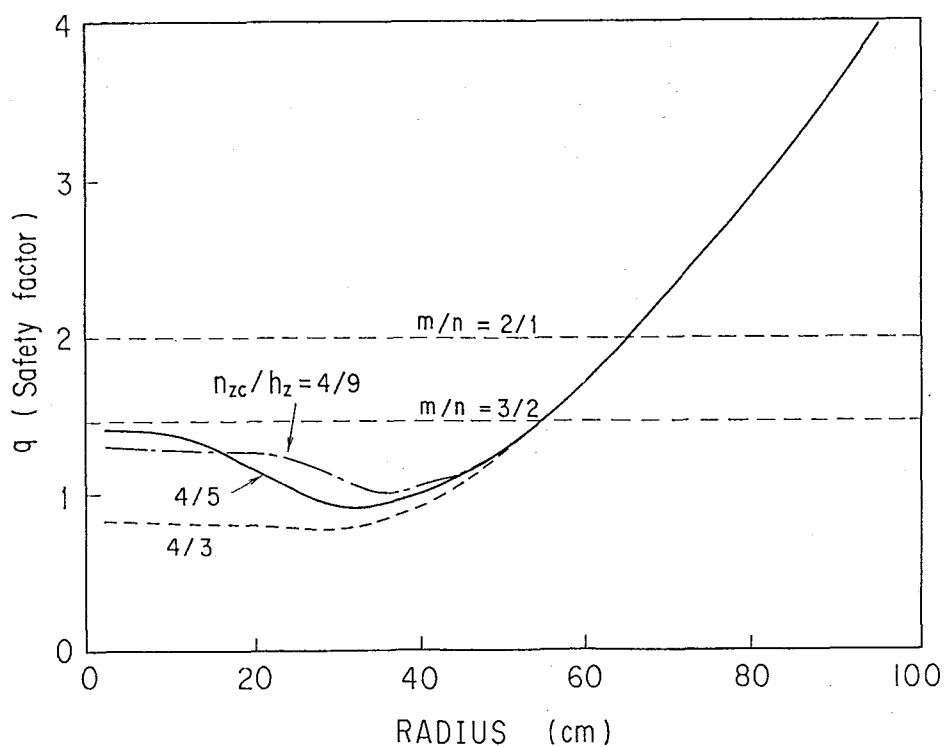


Fig. 6 The  $q$  profile corresponding to Fig.4, in which the case of  $n_{zc}/h_z=4/3, 4/5$  and  $4/9$  are included.

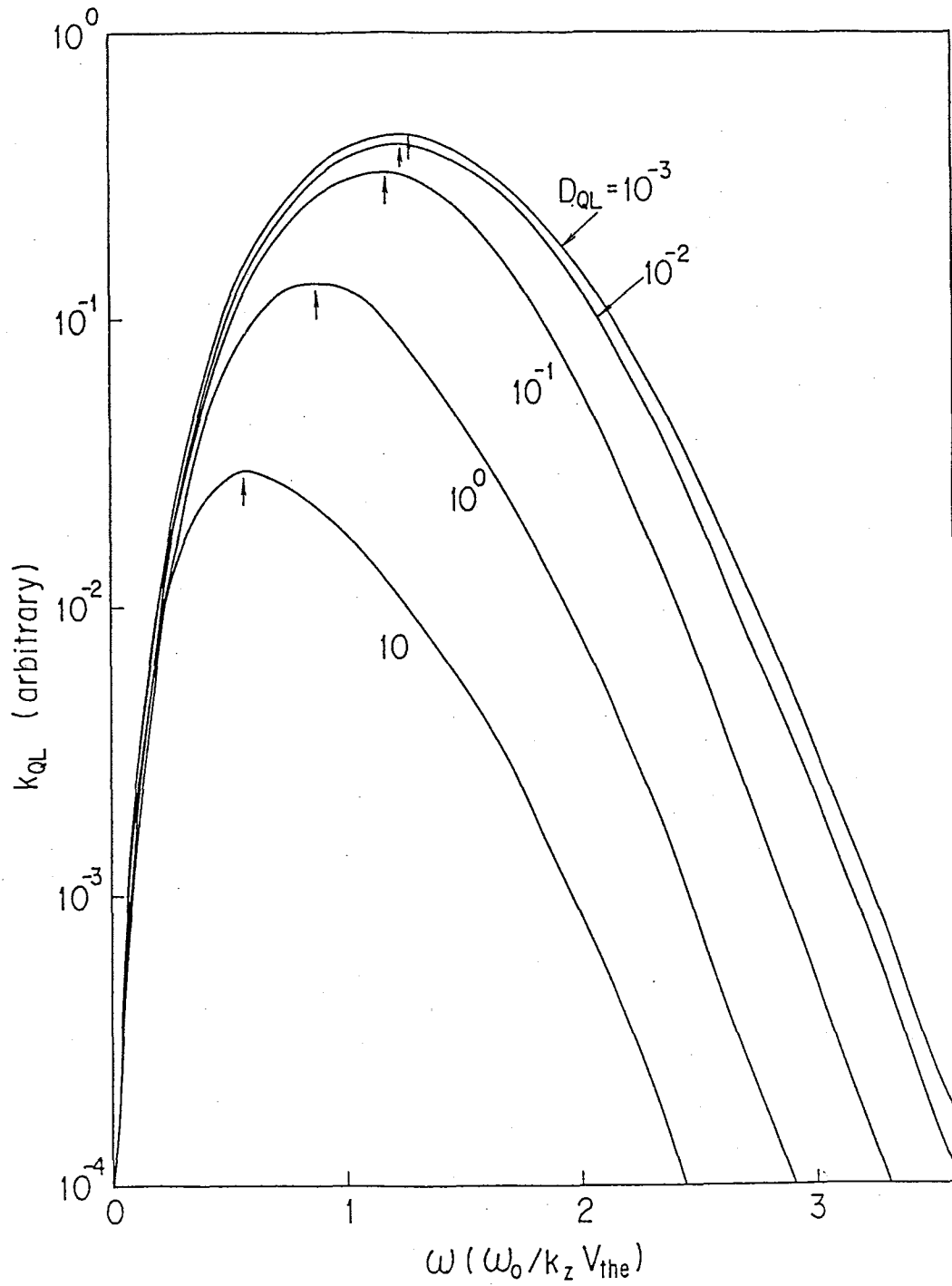


Fig. 7 Schematic drawing of  $k_{QL}$  against  $\omega$ . Signs by arrows are the point  $\partial k_{QL} / \partial r = 0$ .

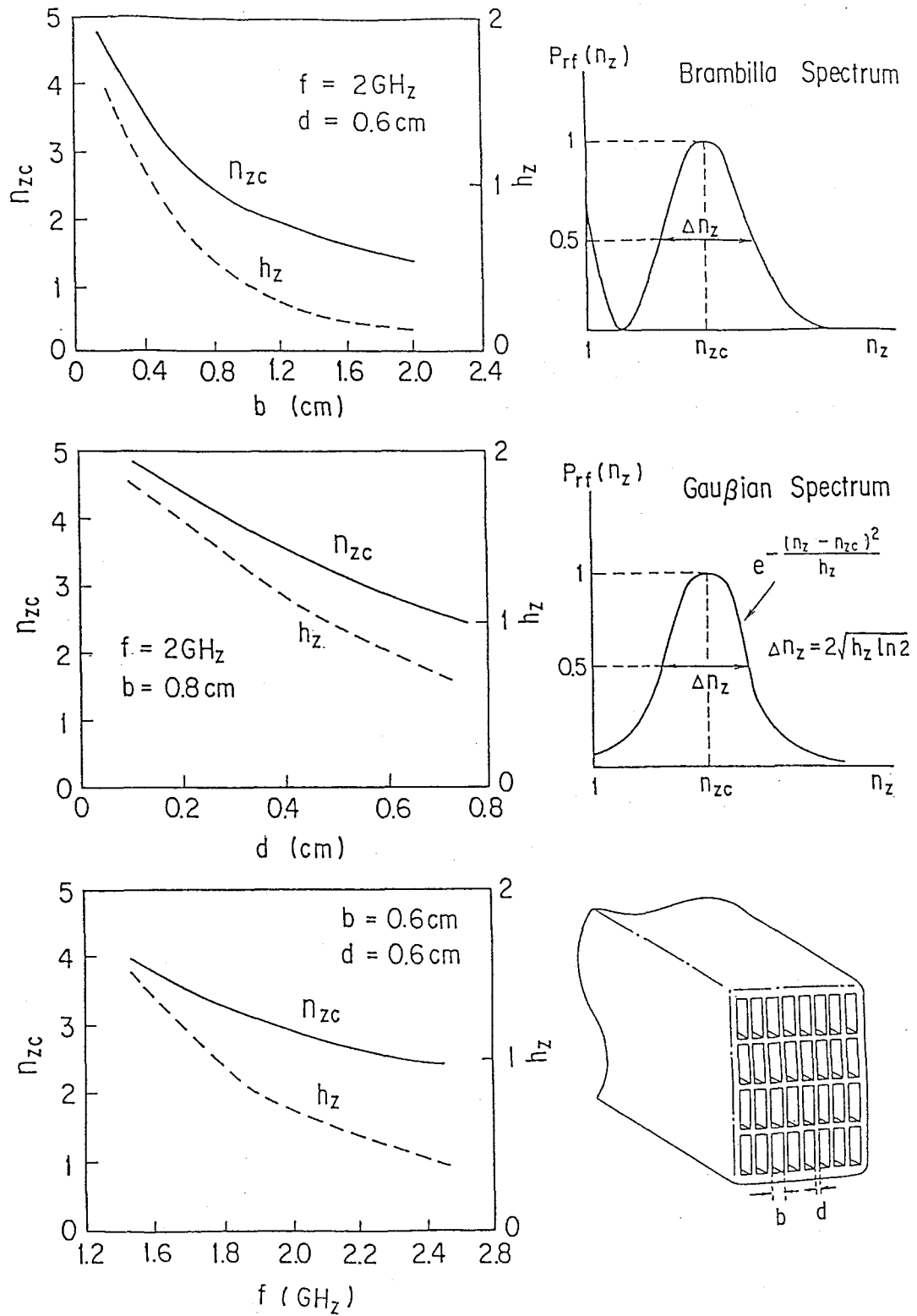


Fig. 8 Relation of Brambilla spectrum and the Gaussian spectrum. The value of  $n_{zc}$  and  $h_z$  against  $b$ ,  $d$ ,  $f$  are calculated in JT-60 lower-hybrid launcher, respectively.

Table 1 Judgment of the major disruption in NICD tokamak. “YES” denotes no major disruption and “NO” does major disruption.

$n_{zc}$	$h_z$	JUDGEMENT
4	3	YES
4	7	NO
4	9	NO
4	11	NO
2	5	YES
3	5	YES
4	5	YES
5	5	YES
3	3	YES
3	5	YES
3	7	YES
3	9	YES